Nuclear Instruments and Methods in Physics Research A 1069 (2024) 169887

Contents lists available at ScienceDirect

Nuclear Inst. and Methods in Physics Research, A

journal homepage: www.elsevier.com/locate/nima

Distillation and gas stripping purification plants for the JUNO liquid scintillator

C. Landini [a,*], M. Beretta [a], P. Lombardi [a], A. Brigatti [a], M. Montuschi [b,c], S. Parmeggiano [a], E. Percalli [a], G. Ranucci [a], V. Antonelli [a], D. Basilico [a], B. Caccianiga [a], C. Coletta [a], M.G. Giammarchi [a], L. Miramonti [a], A.C. Re [a], P. Saggese [a], M.D.C. Torri [a], S. Aiello [d], G. Andronico [d], A. Barresi [h], A. Bergnoli [e], M. Borghesi [h], R. Brugnera [f], R. Bruno [d], A. Budano [g], A. Cammi [k], V. Cerrone [f], R. Caruso [d], D. Chiesa [h], C. Clementi [i], S. Dusini [e], A. Fabbri [g], G. Felici [j], A. Garfagnini [f], N. Giudice [d], A. Gavrikov [f], M. Grassi [f], R.M. Guizzetti [f], N. Guardone [d], B. Jelmini [f], L. Lastrucci [f], I. Lippi [e], L. Loi [k], C. Lombardo [d], F. Mantovani [b,c], S.M. Mari [g], A. Martini [j], M. Nastasi [h], D. Orestano [g], F. Ortica [i], A. Paoloni [j], F. Petrucci [g], E. Previtali [h], M. Redchuck [e], B. Ricci [b,c], A. Romani [i], G. Sava [d], A. Serafini [f], C. Sirignano [f], M. Sisti [h], L. Stanco [e], E. Stanescu Farilla [g], V. Strati [b,c], A. Triossi [f], C. Tuve' [d], C. Venettacci [g], G. Verde [d], L. Votano [j]

[a] INFN, Sezione di Milano e Università degli Studi di Milano, Dipartimento di Fisica, Italy
[b] INFN, Sezione di Ferrara, Italy
[c] Università degli Studi di Ferrara, Dipartimento di Fisica e Scienze della Terra, Italy
[d] INFN, Sezione di Catania e Università di Catania, Dipartimento di Fisica e Astronomia, Italy
[e] INFN, sezione di Padova, Italy
[f] INFN, sezione di Padova e Università di Padova, Dipartimento di Fisica e Astronomia, Italy
[g] INFN, sezione di Roma Tre e Università degli Studi Roma Tre, Dipartimento di Fisica e Matematica, Italy
[h] INFN, Sezione di Milano Bicocca e Dipartimento di Fisica Università di Milano Bicocca, Italy
[i] INFN, Sezione di Perugia e Università degli Studi di Perugia, Dipartimento di Chimica, Biologia e Biotecnologie, Italy
[j] Laboratori Nazionali dell'INFN di Frascati, Italy
[k] INFN, Sezione di Milano Bicocca e Dipartimento di Energetica, Politecnico di Milano, Italy

ARTICLE INFO

Keywords:
LAB
Liquid scintillator
Purification
Distillation
Stripping
JUNO

ABSTRACT

The optical and radiochemical purification of the scintillating liquid which will fill the detector of the JUNO experiment plays a crucial role in achieving its scientific goals. Given its gigantic mass and dimensions, and an unprecedented target value of about 3 % at 1 MeV in energy resolution, JUNO has set severe requirements on the parameters of its scintillator, such as attenuation length ($L_{at} > 20$ m at 430 nm), light yield, and content of radioactive contaminants (^{238}U, $^{232}Th < 10^{-15}$ g/g). To accomplish these needs, the scintillator will be processed using several purification methods, including distillation under vacuum and gas stripping, carried out in two large-scale plants installed at the JUNO site.

In this paper, the layout, operating principles, and technical aspects which have driven the design and construction of the distillation and gas stripping plants are reviewed. The distillation is effective in enhancing the optical properties and removing high-boiling radioactive impurities (^{238}U, ^{232}Th, ^{40}K), while the stripping process exploits pure water steam and high-purity nitrogen to extract gaseous contaminants (^{222}Rn, ^{39}Ar, ^{85}Kr, O_2) from the scintillator. The plant operating parameters have been tuned during the recent commissioning phase at the JUNO site and several quality control measurements and tests have been performed to evaluate the performances of the plants. Preliminary results on the efficiency of these purification processes will be shown.

* Corresponding author.
E-mail address: cecilia.landini@mi.infn.it (C. Landini).

https://doi.org/10.1016/j.nima.2024.169887
Received 7 June 2024; Received in revised form 13 September 2024; Accepted 14 September 2024
Available online 18 September 2024

1. Introduction

In the research field of neutrino physics, liquid detectors have been widely used to investigate the properties of these weakly interacting particles. Organic scintillators have been chosen as the detection medium by several experiments, such as Borexino [1], KamLAND [2], Daya Bay [3], RENO [4], JUNO [5], and SNO+ [6], and the detector targets in liquid scintillator-based technology can easily reach considerable sizes and masses. Due to their homogeneity, flexible handling, affordability, availability in large quantities, and the possibility of different purification methods, liquid scintillators represent an optimal solution. So far, Borexino and KamLAND above all managed to achieve extraordinary results for radiopurity levels even at the kilotonne scale.

JUNO (Jiangmen Underground Neutrino Observatory) is a new-generation liquid-scintillator reactor antineutrino experiment, currently under construction in an underground laboratory (700 m vertical overburden) near Kaiping, Guangdong province, in southern China. The primary goal is the determination of the neutrino mass ordering at $3\,\sigma$ level in 6 years, by detecting reactor antineutrinos from two nuclear power plants, located approximately 53 km away. The gigantic central detector (CD) is composed of a transparent acrylic sphere of 35.4 m in diameter and is designed to contain about 20 000 tonnes of liquid scintillator (LS). 17 612 large (20″) photomultipliers and 25 600 small (3″) photomultipliers (PMTs) installed around the acrylic vessel will detect the scintillation light produced inside, providing a large total coverage of about 78%. These features are designed to reach an unprecedented energy resolution for a liquid scintillator detector of about 3% at 1 MeV (at $1\,\sigma$). The CD is immersed in a high-purity water pool, aiming to shield the active region from the natural radioactivity of the external environment and acting also as a muon veto detector, together with the top tracker [7], to reject cosmic rays background.

To accomplish the extensive scientific program of JUNO [8–12], a high sensitivity and an extremely low background [13] are mandatory. For this purpose, one of the crucial tasks is the purification of the liquid scintillator, which is pivotal for achieving the optical and radiopurity levels required. Indeed, if radioisotopes are present in the scintillating mixture, their signals will be detected, superimposing on the real neutrino signal. Additionally, optical impurities [14] could spoil its transparency, affecting light propagation and detection, and hence the overall energy resolution. Several chemical techniques are available to purify liquid scintillators, but the challenging needs of frontier neutrino physics research imply special attention and a strong push forward in technological and engineering solutions beyond the state-of-the-art.

In the following, the purification strategy of JUNO will be presented, paying particular attention to the distillation and gas stripping purification processes.

The layout of this paper is organized as follows. Section 2 briefly introduces the JUNO liquid scintillator and its purification strategy. The description of the distillation and stripping plants is shown and discussed in Section 3. Finally, plant commissioning and preliminary purification results are given in Section 4.

2. JUNO liquid scintillator

The scintillator of JUNO is based on an organic solvent, the linear alkyl benzene (LAB), whose formula can be written as $C_6H_5C_nH_{2n+1}$, with n typically between 10 and 14. The fundamental part of the molecule is the benzene ring, which can be excited by ionizing radiation, thus assuring the scintillating feature. Given the low costs and the possibility of huge-scale mass production, high transparency and compatibility with acrylic, and good properties in terms of safety and health hazards, the LAB represents an optimal choice as a solvent. The 2,5-Diphenyloxazole (PPO) is added to it as a primary wavelength shifter, to enable the scintillation light emission, while the 1,4-Bis (2-methyl styryl) benzene (bis-MSB) has been selected as a secondary wavelength shifter, to further reduce self-absorption and optimize the coupling with the PMTs in the wavelength region of their highest sensitivity, i.e. around 430 nm.

The JUNO scintillating mixture was optimized through a dedicated test campaign at the Daya Bay laboratories [15], where different concentrations of PPO and bis-MSB were added and studied. The final JUNO LS recipe was set to contain 2.5 g/L of PPO and 3 mg/L of bis-MSB. Also, the liquid scintillators of the SNO+ and Daya Bay experiments are based on the same chemicals, but with different concentrations: the former uses 2 g/L PPO [16], while the latter consists of 3 g/L PPO and 15 mg/L bis-MSB, plus the addition of Gd [17].

The experimental goals of JUNO impose several requirements on the LS, mainly in terms of optical and radiopurity features. Since a low background is mandatory for JUNO to unravel rare neutrino events, the content of radioactive impurities and radioisotopes dissolved in the scintillator must be minimized to prevent undesired signals. Typically, the main sources of contamination, that could be naturally present in the scintillator or introduced from the external environment (dust, air, residual microparticles washed off and/or emanated from surfaces contacted with liquid), are ^{238}U, ^{232}Th, ^{40}K as heavy impurities and ^{222}Rn, ^{85}Kr and ^{39}Ar as gaseous impurities. The minimum radiopurity levels in JUNO are set for the detection of antineutrinos from the two nearby nuclear power plants, in particular ^{238}U, ^{232}Th $< 10^{-15}$ g/g and ^{40}K $< 10^{-16}$ g/g. Instead, for solar neutrino studies, the levels must be even lower at 10^{-16} g/g, or better for measurement with improved precision. Even at 10^{-16} g/g, we foresee improving the Borexino's measurements for ^{7}Be neutrinos in 1 year of data taking and for neutrinos from the CNO cycle in 6 years of data taking [18], which is the same acquisition time needed to determine the neutrino mass ordering at $3\ \sigma$ level. In general, the optimal levels for ^{238}U / ^{232}Th / ^{40}K impurities would be less than 10^{-17} g/g, established as the final target value in JUNO. More details about JUNO radiopurity requirements are reported in Table 1.

Concerning the optical requirements, the transparency and the attenuation length must be carefully controlled to maintain optimal light propagation [19] and thus a good energy resolution. Given the huge dimensions of the central detector (35.4 m in diameter), the optical path of the scintillation light before reaching the PMTs outside could be very long. Hence, the requirement on the attenuation length of the final scintillator mixture is fixed to be $L_{at} > 20$ m at 430 nm. Examples of optical contaminants in commercial LAB may include fused ring compounds, such as naphthalene and its derivatives, biphenyl compounds, diphenyl alkanes, and oxidized organic molecules resulting from oxygen exposure. These could cause absorption peaks in the 350–450 nm wavelength band and, thus, lower transmittance and attenuation length. The LAB for JUNO is a custom-made production by Jinling Petrochemical Co. Ltd, with a reduced content of optical impurities, which will be anyhow removed by Al_2O_3 filtration and distillation processes with JUNO purification systems.

The JUNO LS light yield is expected to be around 1500 p.e./MeV, leading to an unprecedented energy resolution of 3% at 1 MeV. The energy response linearity and the long-term stability with aging are other important features to be considered.

To satisfy all the stringent requirements of the JUNO LS, an accurate multi-step purification procedure for the scintillator has been studied and implemented. This procedure is described in the next subsection.

2.1. Purification strategy for the JUNO LS

As done in other neutrino experiments based on liquid detectors, a purification procedure with multiple chemical processes is crucial to suppress the background from contaminants present in the scintillator itself and improve its radiopurity. Borexino [20], KamLAND [21,22] and SNO+ [23] successfully completed the purification of their scintillators using several techniques, with Borexino achieving the best results to date for ^{238}U and ^{232}Th, measured to be $< 9.4 \cdot 10^{-20}$ g/g and $< 5.7 \cdot 10^{-19}$ g/g respectively [24]. To leverage prior experiences with scintillator purification, JUNO inherited and employed a concept

Table 1
List of the main radio-contaminants that can be present in JUNO liquid scintillator, the relative contamination sources and their typical values. In the last two columns are shown the different requirements for the minimum and the ideal radiopurity scenarios for the JUNO LS.

Radioisotope	Contamination source	Typical value	JUNO requirement	
			Minimum	Ideal
^{222}Rn	Air and emanation from material	$<100\,Bq/m^3$	$<250\,mBq/m^3$	$<5\,mBq/m^3$
^{238}U	Dust suspended in liquid	$\sim10^{-6}$ g/g	$<10^{-15}$ g/g	$<10^{-17}$ g/g
^{232}Th	Dust suspended in liquid	$\sim10^{-5}$ g/g	$<10^{-15}$ g/g	$<10^{-17}$ g/g
^{40}K	Dust suspended in liquid, PPO	$\sim10^{-6}$ g/g	$<10^{-16}$ g/g	$<10^{-18}$ g/g
^{39}Ar	Air	$\sim1\,Bq/m^3$	<50 μBq/m^3	<50 μBq/m^3
^{85}Kr	Air	$\sim1\,Bq/m^3$	$<4\cdot10^{-24}$ g/g	$<8\cdot10^{-26}$ g/g

design for purification systems similar to Borexino, including cleaning procedures, leak tightness, and other technical features.

The JUNO purification strategy involves processing the LS through a sequence of five main purification systems [25]:

1. filtration of raw LAB through Al_2O_3 (alumina) powder, in order to improve its optical properties, increase the attenuation length and smoothen the absorption spectrum [26];
2. distillation of LAB under vacuum, useful to further enhance its optical properties and remove species with a higher boiling point and lower volatility compared to LAB, such as ^{238}U, ^{232}Th and ^{40}K;
3. acid washing with a 5% nitric acid solution followed by two high-purity water washings of the Master Solution, which is a concentrated solution of PPO and bis-MSB in LAB, and then dilution until the JUNO recipe [27];
4. water extraction of LS, which is effective in removing polar contaminants and ions that may contain ^{40}K, ^{238}U and ^{232}Th chain isotopes and daughters[1] [28];
5. gas stripping of LS, in order to extract O_2 and radioactive gases, such as ^{222}Rn, ^{39}Ar, and ^{85}Kr.

For each of these steps, a dedicated large-scale plant has been built and installed at the JUNO experimental site. After completing the first three processes overground, the LS is sent to the underground laboratory by a DN50 stainless steel pipe through the 1.5 km slope tunnel, for the last two steps of the sequence. In case of unqualified samples or if the LS already filled in the CD needs to be re-purified during JUNO's lifetime, it can be sent back and re-processed underground by water extraction and stripping plants. Indeed, these are the only two techniques allowed once PPO and bis-MSB have been added to the scintillating mixture.

3. Distillation and stripping plants overview

Among the complex JUNO LS purification procedure described in Section 2.1, this paper focuses on the details and performance of distillation and stripping purification plants (steps 2 and 5 of the sequence, respectively), which were entirely designed and built in Italy in collaboration with Polaris Engineering company, Misinto (MB), Italy. The full-scale plant design was optimized and finalized with the experience gained during the manufacturing and commissioning of two small-scale pilot plants, installed at the Daya Bay laboratories [29].

All the plants have been realized in compliance with both Chinese and European standards and safety rules.

3.1. From pilot to full-scale plants

In order to study the feasibility and the purification efficiency of these techniques on a LAB-based liquid scintillator, dedicated small-scale pilot plants were realized and installed at the Daya Bay Neutrino Laboratory, near Shenzhen, China. For the distillation and stripping processes, the research and design phase began in 2014, involving INFN (Istituto Nazionale di Fisica Nucleare) and Polaris Engineering in close cooperation. Given the limited budget, the dimensions of each pilot plant were relatively small, fitting entirely in one 2.15 m × 2.4 m × 7 m skid, also for convenience of transportation and handling, and with a maximum flow rate of only 100 kg/h for the purified stream.

After construction was completed in 2016, the pilot plants were shipped to China by sea and installed at Daya Bay. The commissioning and intensive test campaign were carried out in 2017–2018.

The idea was to test the purification techniques and develop a deep know-how that would have been fundamental for the optimization of the process parameters in the full-scale plants. All the details of these pilot plants can be found in [29].

The essential components required for the two processes were implemented, but the level of plant automation was limited to a few automatic valves and controllers for cost-effectiveness. This aspect has been robustly upgraded in the final plants, thus assuring a safe and automated system able to run stably and independently in nominal conditions and fail-safe conditions in case of emergencies.

For the circulation of the scintillator, the membrane dosing pumps of the pilot plants have been replaced in the full-scale plants by magnetic-driven centrifugal pumps, more reliable and suitable for higher flow rates, followed by automatic valves to control the flow. Different types of sensors were tested, especially to measure the level and pressure inside the distillation and stripping columns under the harsh conditions of partial vacuum. The number of vacuum pumps has been increased from 1 to 4, to meet the required pumping speed and provide redundancy, thus also allowing maintenance operations without stopping the plant. Several other features have been later improved on the basis of the knowledge acquired in this preparatory phase.

The pilot plants campaign was successfully concluded, yielding excellent results in enhancing the optical and radiopurity features of the JUNO LAB-based scintillator and laying the foundations for the development of the full-scale purification plants, in a profitable and lasting collaboration with Polaris company.

3.2. Distillation plant

The main goal of the distillation plant is the removal of high-boiling impurities from LAB, like heavy metals and particulate that could contain ^{238}U, ^{232}Th and ^{40}K radioisotopes. This process has also been proven effective in enhancing the optical quality of the solvent, mainly the absorbance and the attenuation length in the 340–500 nm range of wavelengths, by removing optical contaminants such as oxidized organic compounds, which have lower volatility compared to LAB.

[1] In the ^{238}U decay chain, ^{210}Po is difficult to be removed efficiently. During fabrication and assembly of the fluid handling systems and of the detector itself, the internal surfaces may be exposed to air containing ^{222}Rn, which decays and deposits ^{210}Pb onto the exposed surfaces. ^{210}Pb accumulates and subsequently ^{210}Bi and ^{210}Po emanate from the surfaces. Furthermore, Po easily makes non-polar or organic compounds that are very difficult to purify from the LS. For this reason, some Po is always present after filling.

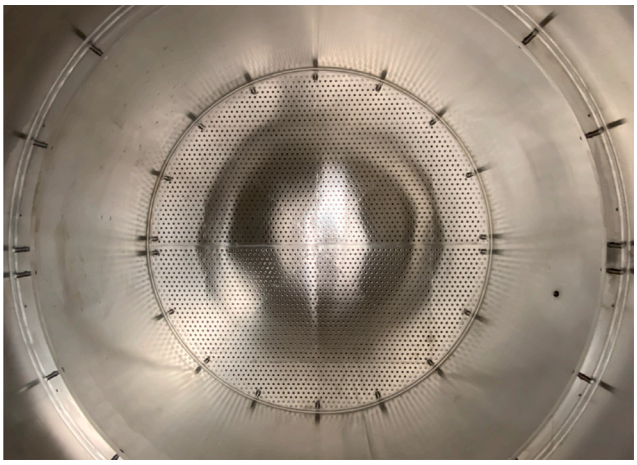

Fig. 1. Installation of sieve trays inside the distillation column.

Fig. 2. Distillation plant installed in the Overground LS building at the JUNO site.

3.2.1. Design and working principles of the distillation column

Fractional distillation is a chemical technique commonly used to separate or extract specific components, known as fractions, from a liquid mixture. Taking advantage of the different boiling points of these fractions, the mixture is heated until selective boiling and subsequent condensation of the desired components occur. The most volatile elements concentrate in a higher percentage in the vapor phase, while the less volatile ones remain in the liquid phase.

In our plant, the distillation process is carried out in a 7 m-high, 2000 mm-wide custom-made distillation column. In the bottom part, a reboiler heated by diathermal oil is directly connected to the column to boil the LAB and produce purified vapors, which are then collected and liquefied at the top of the column by a condenser.

The column is equipped with 6 sieve trays (dual flow trays) with ∼3500 holes (12 mm in diameter), where a layer of liquid can build up, establishing intimate contact with the upward stream of vapors. The purification process is driven by both heat and mass transfers between the gas and liquid phases at each tray, thus forming multiple equilibrium conditions along the height of the column. The vapor and liquid fluxes should be limited to the design operating range so that a suitable contact surface and time at each stage can be ensured.

The distillation of LAB is performed at 210–220 °C in a partial vacuum (60 mbar at column bottom) in order to reduce its boiling temperature, thus avoiding risks of thermal degradation and increasing the separation capability towards high-boiling impurities. For comparison, the LAB boiling point at atmospheric pressure would have been around 300 °C, also very close to the auto-ignition temperature (295–330 °C).

The vacuum level inside the column is kept constant by 4 parallel vacuum pumps (VPs) connected in the upper part, after the condenser (see Fig. 3). Pressure is the key operating parameter that drives all the others inside the column and should be set carefully at the top and bottom ends to ensure good performance and purification efficiency. The pressure at the condenser is automatically adjusted to approximately 5 mbar by VPs through a regulating valve. The bottom pressure, at the reboiler, determines the boiling temperature of the liquid, which always remains constant during phase transitions. The optimal value is designed to be ∼60 mbar and can be controlled by increasing or decreasing the thermal power supplied by the reboiler to the LAB. The pressure difference between the top and bottom values corresponds to the total height of liquid accumulated on the trays: considering 55 mbar of pressure difference and a LAB density of 720 kg/m^3 at 200 °C average temperature, the corresponding height is approximately 78 cm, thus implying a liquid layer of ∼13 cm on each tray. So, in this design, the liquid is held on the perforated tray by the pressure of the lower stage, in a dynamic equilibrium between evaporation and condensation. If pressure changes abruptly, the layers on the trays could break and the liquid would fall to the bottom of the column. Since the height of the liquid layer on the trays affects the global purification efficiency of the distillation process, the pressure values inside the column must be carefully controlled to avoid any destabilization.

The design of the distillation column was driven by several criteria. Among various options, sieve trays were chosen because of their simple but effective layout, since they have no moving parts, can be easily cleaned, and can be mounted inside the column without welding. A picture of them is shown in Fig. 1. The choice of only six stages in the column design was motivated by a good compromise between space availability, plant dimensions, and suitable purification efficiency. The height of the column was constrained by both the height of the building (15 m) and the need to prevent a pressure difference too high between the bottom and top ends, which would have led to an excessive increase in the bottom pressure and the LAB boiling temperature, risking thermal degradation. Instead, the pressure at the top end should be avoided from decreasing further below the mbar level. This is to maintain the specific volume of the vapors and the vapor velocity inside the transfer line from the column head to the condenser at a reasonable level, and to ensure a sufficient vapor–liquid contact time on the highest sieve trays. The calculation for the separation efficiency of the process was based on PPO, as a conservative evaluation for all the optical contaminants and heavy metals with lower volatility, and the minimum number of required stages was found to be between five and six for a separation efficiency close to 98%–99%. All these technical features, together with the desired plant parameters, were taken into account in detailed and complex simulations done by Polaris company to optimize the distillation column design and arrangement, which resulted in the one illustrated in this paper.

3.2.2. Layout of the full-scale plant

The plant is designed to operate at 7 m^3/h of nominal flow rate. A sketch of its flow diagram is reported in Fig. 3, while the main parameters are listed in Table 2. The LAB entering the plant is collected in a 20 m^3 vertical feed tank and pumped to the distillation column to start the purification. The liquid is fed at mid-height, above the third tray, after being pre-heated by two counter-flow heat exchangers at about 180 °C, thus avoiding destabilizations of the column temperature

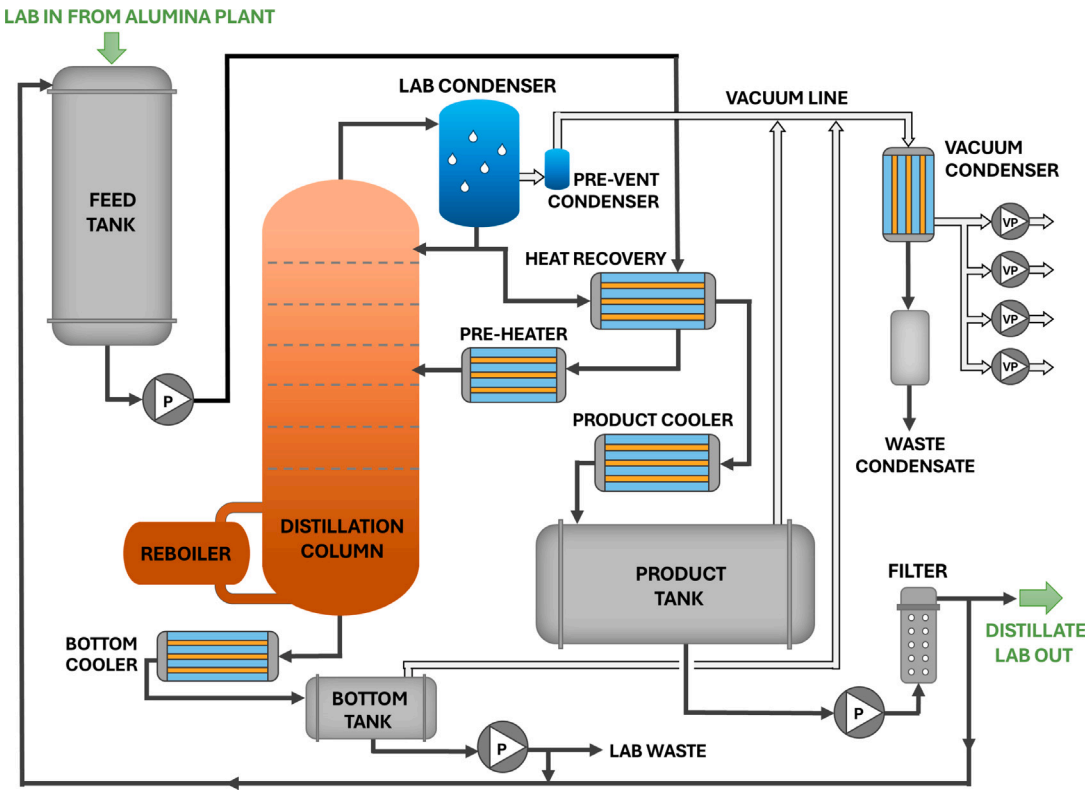

Fig. 3. Flowchart scheme of the distillation plant (not to scale). The input LAB is fed into the feed tank, heated to 180 °C by the heat recovery and the pre-heater and introduced into the column above the 3rd tray, where it falls by gravity in the bottom part. Here it is evaporated by the reboiler at about 210–220 °C. The stream of purified LAB vapors is extracted and condensed in the top part by the condenser and a certain portion (up to 50%) is recirculated to the column as internal reflux. The distilled LAB is then cooled down to ambient temperature by the heat recovery system and the product cooler and stored in the 20 m^3 horizontal tank. The bottom of the column is discarded regularly into the waste bottom tank to remove the contaminants. The pressure inside the distillation column, the product tank and the bottom tank is kept constant at 5 mbar using a set of 4 parallel vacuum pumps (VP). Finally, after being filtered, the distilled LAB can be either pumped out towards the Mixing plant or sent back to the feed tank for internal loop circulation.

Table 2
Main features and operating parameters of the distillation plant.

Distillation plant parameter	Value
Sieve trays	6 trays
Tray holes	3500 holes (12 mm diameter)
LAB nominal flow rate	7 m^3/h
Reflux rate	Up to 50%
Bottom discharge	1–2%
Pressure (at column top)	5 mbar
Temperature @ reboiler	210–220 °C
Heating thermal power	1000 kW_{th}
Heat recovery	400 kW_{th}
Column diameter	2000 mm
Column height	7 m
Plant dimensions	10 m × 9 m × 14 m
Approx. plant weight	55 tonnes

profile. In the first exchanger, the incoming cold LAB is heated up by the distilled hot condensate, enabling heat recovery and energy savings (in the order of 400 kW_{th}); the second heat exchanger, supplied with hot oil, makes the final temperature adjustments in the column feed stream. The liquid, falling by gravity, is collected in the bottom part of the column vessel and boiled by the tube-bundle reboiler, thus generating LAB vapors. High-boiling and low-volatility impurities that accumulate in the unevaporated liquid phase remain in the bottom part and are regularly discarded into a 4 m^3 waste tank every 30 min, up to 2% of the plant nominal flow rate (7 m^3/h), i.e. 140 L/h. This value allows for the progressive separation and disposal of contaminants while limiting LAB waste and costs.

With the experience gained from the pilot plant, the number and type of sensors used to monitor the level of liquid inside the column were increased for redundancy, compared to the pilot plant design. Safe and efficient operation requires the level to be kept within a specific range, to avoid both flooding phenomena and lowering the level below the reboiler. Thus, in the bottom part of the column, the following have been installed: three level switches (Liquiphant S FTL71 by E+H), two of which serve as low-level alarm thresholds and one as a high-level alarm; one differential pressure transmitter (SITRANS P DSIII series by Siemens) and one guided-wave level radar (Levelflex FMP54 by E+H), to measure the height of the liquid level with two different measuring principles simultaneously. Above them, one differential pressure transmitter (SITRANS P DSIII series by Siemens) measures the pressure difference below the lowest tray and above the highest one to calculate the total internal height of liquid accumulated on the trays.

After boiling, purified LAB vapors that rise up inside the column are extracted at the top end and liquefied by a two-phase condenser, supplied with water at ambient temperature from a cooling tower. To further increase the purification efficiency, a fraction of the distilled and condensed liquid stream – up to 50% as an optimal compromise between a balanced throughput and product purity – is immediately reintroduced into the column as reflux. The remaining part is conveyed by gravity to the 20 m^3 product tank, after being cooled down to ambient temperature. For technical needs and plant size optimization, the product tank is arranged horizontally and is kept at the same pressure as the column head. This forced us to place the circulation pump of the LAB product inside a 4.5 m-deep well, dug into the ground floor, to ensure a suitable NPSH (Net Positive Suction Head) at the pump inlet nozzle, to avoid running the pump dry and preventing cavitation phenomena. The pump pushes the purified LAB through a set of 50 nm filters as a final step, with the purpose of retaining any dust or microparticles that may have been washed off the surfaces.

Finally, the distilled LAB can be either sent forward to the Mixing plant or circulated back to the distillation inlet feed tank for further purification in internal loop mode.

The plant is equipped with 4 vacuum Roots pumps, to keep a constant pressure of 5 mbar at the column head and inside the product and the bottom tanks. The VPs are preceded by a vent condenser, which condenses and removes any LAB droplet from the uncondensable gases sucked by the vacuum pumps. Since in the pilot plant was observed that some LAB vapors could anyway reach the VP, especially during the start-up phase, in the full-scale plant a small pre-vent condenser was added to the vacuum line near the column head.

Each component is supplied with a continuous stream of nitrogen (N_2) as cover gas blanketing and purge to avoid oxidation of the LAB.

The distillation plant is now installed in the Overground LS building at the JUNO site (Fig. 2). It was built and pre-assembled in Polaris's workshop, constructed as six skids plus one vertical tank and one horizontal tank, and then shipped to China by sea. Due to its large size, the installation was performed from the roof of the building using a 120 tonnes truck crane.

3.3. Stripping plant

The stripping plant is the final stage of the purification procedure for the JUNO LS. Gas stripping process is used to remove gaseous impurities naturally dissolved in the scintillator, mainly ^{222}Rn, ^{85}Kr, and ^{39}Ar radioisotopes, which could generate undesired background signals, and O_2, that is responsible for photon quenching and oxidation in the LS. Moreover, the stripping process can also remove possible dissolved water left during the water extraction process.

3.3.1. Design and working principles of the stripping column

Gas stripping is a gas-liquid separation process where gases dissolved in a liquid phase are extracted by desorption mechanisms, exploiting a stream of pure stripping gas. This purification technique relies on Henry's law, which states the dependency of the amount of a gas i in a liquid being proportional to its partial pressure (i.e. the left side of Eq. (1)):

$$y_i \cdot p_t = K_{H,i} \cdot x_i \tag{1}$$

x_i and y_i are the molar fraction of i in liquid and gas phases respectively, p_t the total pressure and K_H the Henry's constant in atm units. The latter depends on temperature; therefore, changing this operational parameter can affect purification efficiency.

The process is based on the mass transfer of the contaminant i in the liquid phase passing to the vapor phase, i.e. the stripping gas. The molar flow rates of gas (G) and liquid (L) streams determine the operating conditions of the process and the so-called stripping factor S [30]:

$$S = \frac{L \cdot K_H}{G \cdot p_t} \tag{2}$$

This quantity represents the removal rate of the contaminant between two equilibrium stages. As can be easily inferred from S, the process becomes more efficient at lower pressure p_t, due to a decrease of the gas solubility in the liquid phase x_i, according to Henry's law (Eq. (1)). The stripping efficiency also increases at higher temperatures, as this directly raises Henry's constant K_H.

Our plant is equipped with a 9 m-high custom-made vertical stripping column filled with unstructured packing, i.e. AISI316 stainless steel Pall rings of 13 mm diameter (specific interface area $a = 430\,m^2/m^3$; see Fig. 4). The packing is inserted with the purpose of spreading the liquid in thin films or drops, thus increasing the contact surface between the two phases. Actually, the mass transfer directly depends upon the interface surface exposed between gas and liquid phases: the larger this parameter, the higher the purification efficiency. Ultrasonic bath cleaning, carried out at 60 °C in a demineralized water solution with 3% Alconox detergent, was adopted to cleanse the Pall rings before assembling and filling the column.

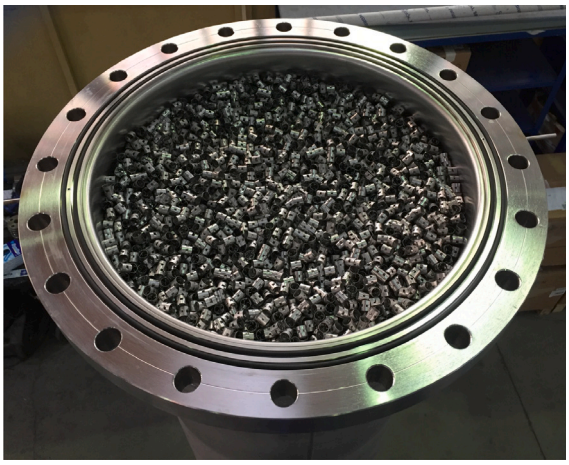

Fig. 4. Filling of the stripping column with unstructured packing of Pall rings (patented device, cylindrical shape with a diameter of 13 mm, stainless steel).

The purification process is performed in counter-current flow mode, feeding the LS from the top and the gas from the bottom. At the top and middle height, the column features a distributor tray, which restores a uniform spatial distribution of liquid flux within.

The stripping gas consists of an adjustable mixture of high-purity nitrogen (HPN, up to 50 Nm^3/h) and ultra-pure water steam (UPW, up to 30 kg/h). Both HPN and UPW are produced in two dedicated plants at the JUNO site, to ensure optimal quality and purity in terms of Rn, Kr and other radioisotopes; this is important because their residual content sets the purification limit that can be reached in the stripping process. The HPN system [31] exploits low-temperature adsorption (LTA) technology to achieve $^{222}Rn < 5\,\mu Bq/m^3$ and $^{85}Kr < 10\,\mu Bq/m^3$. UPW, with resistivity $> 18\,M\Omega \cdot cm$ and $^{222}Rn \leq 7\,mBq/m^3$, is obtained with a complex pure water system [32], which includes several degassing membranes and devices.

The stripping plant is designed to operate in a partial vacuum, at about 250–300 mbar, and up to 90 °C: this increases the stripping efficiency, as explained before from Eqs. (1) and (2), and reduces the LS viscosity, further optimizing the spreading inside the column packing and the exchange with the stripping gas.

In the Daya Bay tests, the stripping process was performed only with HPN at 90 °C and 300 mbar: a purification efficiency of 95.8% for ^{222}Rn was obtained on a 115 L/h LS flow rate using a stream of 1 N m^3/h HPN. The dimensions of the column were scaled up to design the final plant for JUNO, but the height has been further increased by 50%. Based on simulations for Rn removal, the full-scale plant is expected to have between 3 and 4 theoretical stages and about 95% of efficiency for a LS flow rate of 7000 L/h, with 15 Nm^3/h HPN as stripping gas. For lighter gases, the efficiency is anticipated to be even better, e.g. about 99% for O_2. This simulation is based on utilizing only HPN as a stripping gas. As will be explained in Section 4, stripping with UPW will turn out to be impracticable for transparency issues with JUNO LS.

3.3.2. Layout of the full-scale plant

The design and layout of the plant are based on a nominal LS flow rate of 7 m^3/h. The flow diagram and the operating parameters are reported in Fig. 5 and Table 3, respectively.

The LS, delivered by the Water Extraction plant, is collected in the 20 m^3 vertical feed tank and pumped through a first set of 50 nm filters, to prevent dust from previous stages or transfer pipelines from polluting the internal surfaces and the column packing. The scintillator is heated

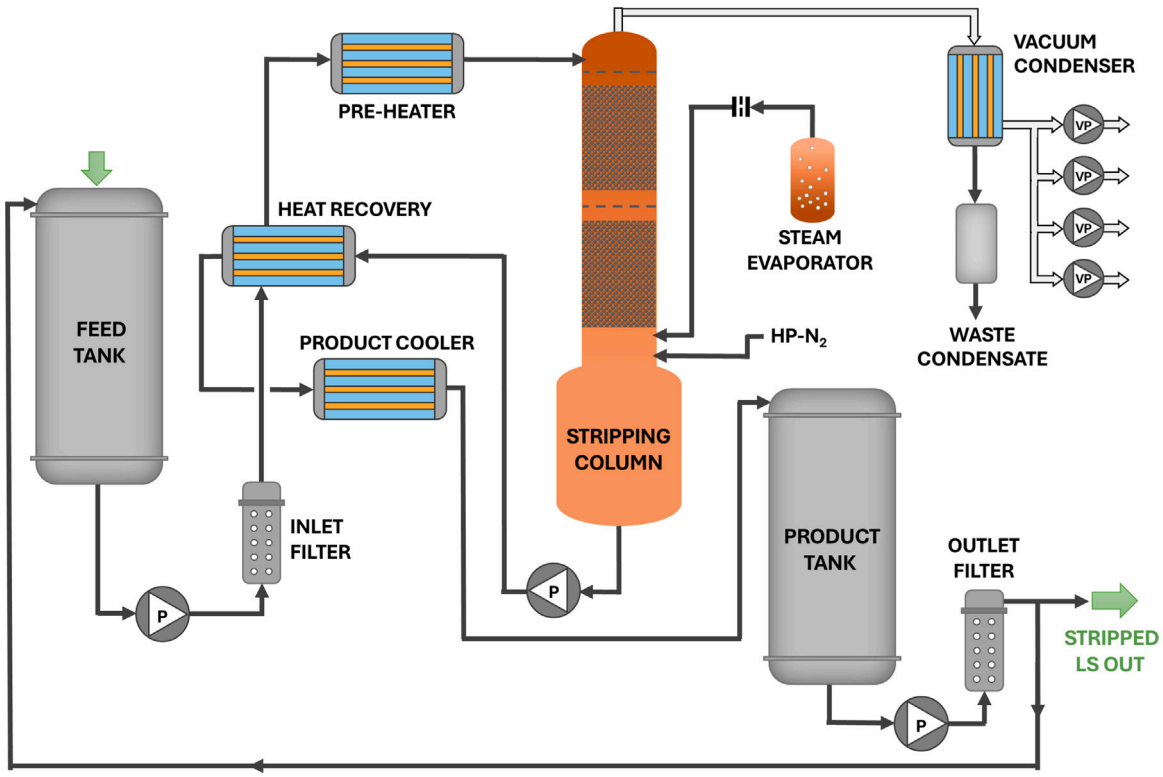

Fig. 5. Flowchart scheme of the stripping plant (not to scale). The LS entering the plant is pumped from the 20 m^3 feed tank through the inlet filters and heated by the heat recovery and the latter heat exchanger. The LS is then introduced into the stripping column from the top, falling by gravity, while the stripping gas, an adjustable mixture of high-purity nitrogen and ultra-pure water steam, is fed from the bottom. The purified LS is collected at the bottom of the column, cooled down to 21 °C and stored in the product tank. Finally, it is filtered by passing through the outlet filters and it can be pumped either to the next stage or sent back to the feed tank for internal loop circulation. The vacuum level inside the column is kept constant by a system composed of a vacuum condenser and 4 parallel vacuum pumps.

Table 3
Main features and operating parameters of the stripping plant.

Stripping plant parameter	Value
Column filling	Unstructured (Pall-rings)
Pall-rings diameter	13 mm
Specific interface area	430 m^2/m^3
LS nominal flow rate	7 m^3/h
HPN flow rate	Up to 50 Nm^3/h
UPW steam flow rate	Up to 30 kg/h
Pressure	250 mbar
Temperature	70–90 °C
Heating thermal power	200 kW_{th}
Heat recovery	160 kW_{th}
Column diameter	500 mm
Column height	9 m (5.6 m of packing)
Plant dimensions	6.5 m × 9 m × 12 m
Approx. plant weight	35 tonnes

to the desired process temperature before being supplied to the column head. Similarly to the distillation plant, we take advantage of heat recovery from the stripped hot scintillator in the first heat exchanger, while the second one adjusts the temperature to the target value.

The falling LS is contacted and stripped by the upward stream of the gas mixture. The two gases are injected by two separate nozzles at the column bottom, below the unstructured packing. HPN is supplied by the HPN system and the injected flow can be precisely controlled by a needle valve. The water steam (30 kg/h maximum) is generated starting from UPW, which is evaporated at about 250 mbar (boiling temperature ∼65 °C) inside a steam generator supplied with diathermal oil at 120 °C. Given the long time contact inside it, the steam is produced superheated and dry and is transferred to the stripping column via a pipeline wrapped in heating belts, to maintain the vapor temperature and prevent recondensation. A calibrated orifice of 1 cm in diameter controls the UPW steam flux injected into the column.

After being stripped, the LS is cooled down to 21 °C and stored in the 20 m^3 vertical product tank. The final step is the filtration through another set of 50 nm filters, that restrain any dust or metallic particulate that could have been released by the Pall rings or other surfaces. The purified LS can be either sent to the Central Detector of JUNO for its filling procedure or recirculated back to the stripping inlet feed tank for internal operation, in case of need.

A set of 4 parallel vacuum pumps is connected to the column head to maintain a constant pressure of 250 mbar at that point and to remove the exhausted stripping gas from the column. A slight pressure gradient of about 10–15 mbar is observed along the column, from the top to the bottom end. Condensable vapors, such as water steam, flowing towards the VPs are liquefied and drained by a vent condenser placed just before them, while the non-condensable vapors, such as nitrogen, are expelled by the pumps themselves.

The stripping plant is installed in the Underground LS Hall at the JUNO site. It is composed of 2 vertical tanks and 3 skids, with 5 walkable floors in total. Each unit has been transported to the underground laboratory through the 1.5 km slope tunnel and assembled using the overhead crane installed on the LS Hall roof. A picture of the stripping plant is shown in Fig. 6.

3.4. Common features

Some common criteria and concepts have driven the design and production of these two plants.

3.4.1. Cleanliness and air tightness requirements

Several additional precautions have been adopted in order to achieve the desired LS purity and avoid spoiling it.

Fig. 6. Stripping plant installed in the Underground LS Hall at the JUNO site.

316L stainless steel was selected for manufacturing all main components of the plant and any parts that come into contact with the scintillator. In addition, a special cleaning procedure was studied and implemented to treat the surfaces and prevent oxidation phenomena: a mirror finishing of the steel through electropolishing below 0.8 μm; acid pickling and degreasing of the welds; mild passivation to create an inert layer, using a solution of 25% nitric acid and 75% demineralized water; rinsing with water until conductivity and pH values were restored; compressed air-drying process with dehumidifier and coalescing filters and final storage under N_2 atmosphere. Several quality controls were performed to certify the cleaning procedure, such as particle counting test, endoscopic inspection, and white wipe test. A final rinsing with high-purity water was executed at the JUNO site, after plant installation and skid assembling. The rinsing water was analyzed via particle counting to fulfill MIL-STD-1246C – Class 50 cleanliness level [33].

To maintain the required level also during the run phase, 50 nm pore size pre-wetted filters were installed on the scintillator pipelines, with the aim of preventing circulation of dust and metallic particulate that could be present inside the plants, despite the special cleaning procedure adopted. To allow maintenance operations on filters without forcing a stop of the plant, every filtering stage is composed of two independent filter holders, which allocate six 20″–filter cartridges each. In the distillation plant, filtration is performed as the final step on the outlet line. For the stripping process, filtration occurs both on the inlet line (before the stripping column, to prevent dirt particulates from being trapped in the unstructured packing) and on the outlet line.

Since radioactive gases and oxygen can spoil the LS, the whole plant must be air-tight proof. The layout of the flanges includes double o-ring protection (Viton gaskets for flange exposed to temperatures <150 °C, Kalrez gaskets for higher temperatures). Each component, flange, or moving part has been tested with a helium leak detector to ensure proper sealing. JUNO requirements set the thresholds of $<10^{-8}$ mbar·L/s for single leak rate and $<10^{-6}$ mbar·L/s as overall integral leak rate, according to the calculations to meet the JUNO physics solar program. A plant-wide campaign of He-leak testing certified everything to be within specifications. Moreover, the flanges are continuously purged by a constant flux of HPN, to further reduce any possible air leakage from outside. The flanges have been designed with a custom-made double o-rings layout with purge ports in between.

A procedure of vacuum pumping down to mbar level and nitrogen purging above 1.2 bar has been repeated three times, to remove air and create an inert nitrogen atmosphere before filling the plant with the scintillator. During the operation phase, all tanks and the columns are kept under HPN blanketing, in overpressure (compared to atmospheric pressure) whenever feasible.

3.4.2. Mechanical aspects

All main components and pipelines were pre-assembled and mounted inside skids before shipping them to China. Orbital welding or TIG welding was adopted whenever possible, while interconnections between skids or equipment were fitted with flanges sealed with o-rings. For $\frac{1}{4}''$ sampling ports, VCR fittings with metal gaskets were chosen.

All main pipelines for LS circulation were equipped with full-bore ball valves, while pneumatic regulating valves were installed at crucial points to remotely control the most important plant parameters, such as feed and product fluxes and the pressure in the column.

To improve thermal efficiency, Rockwool was chosen as an insulating material for hot pipelines and equipment, while Armaflex was used for cold ones.

Each plant is provided with 4 vacuum multi-stage Roots pumps (model ACP 28 by Pfeiffer Vacuum), mounted in parallel and located on the upper floors of the plant, near the main column, to keep the design vacuum level during the purification process. 4 parallel pumps were chosen for redundancy, reliability and maintenance reasons: both plants can operate stably with only 3 pumps running, while performing maintenance on the fourth.

The 3 magnetic-driven centrifugal pumps (model UTN-BL 40-25-160 by CDR Pompe s.r.l. company) for the circulation of the scintillator inside the plant are positioned on the ground floor (or even beneath it, in the distillation plant) to ensure stability and a proper NPSH.

Both plants can be operated either in internal loop mode, during self-cleaning, commissioning, and start-up operations, where the liquid is recirculated back to the input feed tank, or in production mode, where the processed scintillator is sent forward to the next stage of the purification sequence.

3.4.3. DCS and automation

The plants are controlled by a reliable and safe Distributed Control System (DCS), which sets the operating parameters, monitors their trend, and actuates an alarm & interlock system in case of out-of-range values or emergency.

It is based on a Siemens PLC, model ET200S, installed in a control panel along with the I/O modules, and it is supervised by a local PC with dedicated SCADA software with a user interface (UI). The PLC communicates with the PC through a MODBUS serial line, while field signals from instruments and sensors are transmitted to the control panel through a 4–20 mA wiring protocol.

The PLC has three main logic areas: the main control functions, always active to monitor the operating parameters and adjust accordingly the automatic valves and items to reach the setpoint value; the automatic sequences, which are set by the operator to be run independently and automatically by the system under certain conditions; the alarms and interlocks, which set the operating and safety ranges for each variable, provide acoustic and visual alarms if the ranges are exceeded, and inhibit some functionalities in case of emergency, up to the shutdown in the worst cases. The interlocks can be software-based, the most common one, where the inhibition is activated by the SCADA software with logic commands (but can also be bypassed in case of need), or hard-wired based, used only for critical items, where the electric signal is physically interrupted by opening the circuit.

The supervision system relies on a user-friendly panel with different pages, that allows an easy and efficient monitoring of the plant. The Run page displays a scheme of the plant, with all the field variables measured in real time. The second page collects a list of all alarm signals that have occurred, both past and ongoing. On the last page, several graphical trends for the main operating parameters are reported: they show the history of values measured during time for each variable and they are crucial to understand the dynamic behavior of the plant.

3.4.4. Safety

The plants have been studied to fulfill several international regulations and certifications and they have received the EC declaration of conformity.

Skid frames and structural loading diagrams are designed to meet both European and Chinese safety regulations. For the JUNO experimental site, all equipment must comply with the National Standard of People's Republic of China Code of Seismic Design of Buildings GB 50011–2001. During calculations, grade VII seismic fortification intensity with a 0.10 g horizontal acceleration was considered.

All tanks, vessels, columns, and main components have been certified according to PED - Group1 - Category IV - Module G classification of PED[2] directive for pressurized equipment. After the construction phase, they underwent both overpressure and vacuum tests. Rupture disks (R-SCR/706 by Donadon SDD S.r.l.) are installed on all tanks and the two columns and are designed to break at 3.5 bar_g, while a pressure safety valve is mounted on the HPN feed line. The plants have also been licensed by the Chinese authority SELO (China Special Equipment Licensing Office).

For fire protection, all electrical equipment is provided with certification for ATEX[3] area classification, in Class 1 Zone 2 T2. Actually, in the distillation plant, the LAB is operating at temperatures above its flash point (130 °C), but anyhow well below the auto-ignition temperature (295–330 °C).

Security lights, active also in case of power outage, have been installed to illuminate any access points and paths.

A detailed Hazop (HAZard and OPerability) analysis for industrial risk assessment was carried out in collaboration with a team of international experts. The major hazards arising from normal and abnormal operations were identified, together with their occurrence probability and severity. Each functional block of the plant was isolated and examined for possible deviations from the design intention. For the hazards, including fire, over-pressures and electrical power failure, actions and systems for prevention and protection were defined and prepared.

4. Commissioning and preliminary results

During an intensive commissioning phase, the distillation and stripping plants have been run repeatedly, first in internal loop mode to test and optimize the operating parameters, then in production mode for the joint commissioning with all the other purification plants. They were operated for more than 8 h uninterruptedly many times, in order to test both the stability and the repeatability of the operating conditions. All parameters were tuned to maintain a production flow rate of 7 m^3/h, which is required to complete the CD filling in 6 months, and all other nominal values, while providing an efficient purification. Both demonstrated excellent stability and safety levels throughout the whole testing period.

For the distillation plant, the condenser for purified LAB vapors after the distillation process represents the most critical component to be set, since the condensed liquid is split between the reflux stream back to the column and the product one, sent to the production tank, that must be kept at nominal 7 m^3/h. Fine adjustments must be made to control both the flow rates and the outlet temperature from the condenser. Subcooling below 100 °C should be avoided to prevent thermal destabilization of the column by the reflux and take advantage of the heat recovery exchanger exploiting the hot product stream. For these reasons, the condenser's cooling power was gradually tuned by carefully regulating its valves, while continuously monitoring the LAB outlet values. The optimal configuration was found to be about 185 °C at the column top, 130 °C as outlet temperature from the condenser, and a reflux flow rate of 4–5 m^3/h. During the entire commissioning, almost 300 m^3 have been distilled in total, to tune all working parameters and gain experience in managing the plant during all phases, from start-up to shutdown.

Concerning the stripping plant, several tests of the stripping purification process were carried out using HPN, UPW steam and a mixture of them, to check feasibility and perform the plant commissioning. When using UPW, some issues emerged due to the solubility levels of water in LAB changing with temperature. Samples extracted at 50 °C or above were initially perfectly transparent, but as the scintillator cooled down to room temperature, the dissolved water in the LAB started to condense, resulting in a milky emulsion of suspended water droplets that temporarily compromised the transparency of the sample. After a recovery period of over 24 h, the LS and water separated, thereby restoring the quality of the former. Nonetheless, it was considered safer to exclusively use nitrogen for the stripping process to prevent excessive water content in the scintillator.

After this effect was pointed out, further investigation also on the water extraction process (refer to step 4 of the purification sequence described in Section 2.1) was performed through a joint commissioning together with the stripping plant. In particular, the removal efficiency of water and the residual water content after the stripping process at different operating temperatures and pressures were tested. The stripping temperature was varied between 70 °C and 90 °C, while the pressure at the column head was tested between 250 mbar and 350 mbar. The water content assay was performed before and after the stripping process with a dedicated apparatus. The best working configuration was determined to be 70 °C at 250 mbar, using 15 Nm^3/h HPN as stripping gas: with these parameters, the water content was reduced from 154 ppm down to 20 ppm, which complies with JUNO standards.

Concerning optical and radiopurity features, to carefully verify the performances and the purification efficiencies of both plants, a comprehensive set of several measurements with different techniques was established, including absorption and emission spectra, particle counting, evaluation of the attenuation length, ICP-MS and NAA. After each plant operation, samples were taken and analyzed to check compliance with the stringent JUNO requirements. The first results of some of them are presented in the following; instead, the results for radioactivity measurements are still preliminary and will be released soon by the JUNO low background group in a dedicated paper.

In Fig. 7, a comparison is reported between the absorption spectra, in arbitrary units a.u., of raw LAB (gray, dotted line), distilled LAB (green, solid line) and stripped LAB+PPO (blue, dash-dot line). The absorption peaks at 370 nm and 390 nm of the gray curve were crucially decreased after the distillation process performed directly on raw LAB, thus proving also the good optical purification capabilities of this plant. Then, the solvent was mixed with PPO, sent underground, and purified by the stripping process, resulting in the blue line: the addition of PPO caused a natural shift of the absorption edge towards longer wavelengths, around 355 nm; however, the rest of the line closely overlaps with the green one, meaning that this process did not affect or introduce significant optical contamination sources into the scintillator, thanks also to the cleaning procedure and leak-tight solutions adopted.

This was further confirmed by the excellent particle counting results, which are reported in Table 5. These values should be compared

[2] Pressure Equipment Directive.
[3] ATmosphere EXplosive.

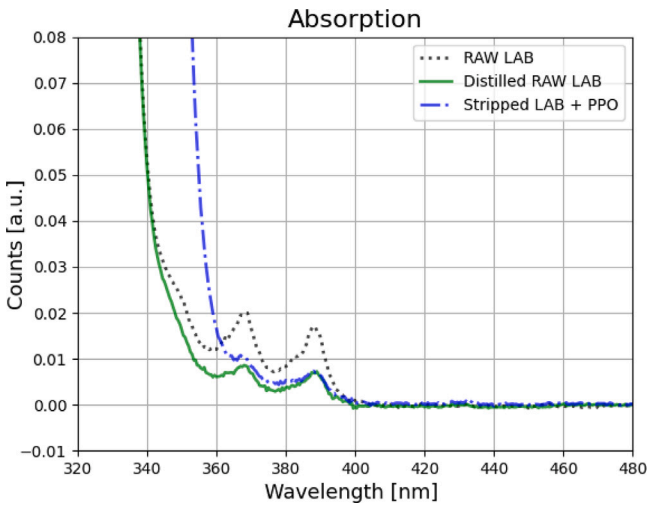

Fig. 7. Absorption spectra, in arbitrary units a.u., of raw LAB (gray, dotted line), distilled LAB (green, solid line) and stripped LAB+PPO (blue, dash-dot line).

Table 4
The MIL-STD-1246C – Class 50 cleanliness level, adopted as the standard reference for JUNO LS: the number of particles must be lower than the threshold value for each particle size.

JUNO Class 50 (from MIL 1246C)	
Particle size (μm)	Count/L
5	1660
15	250
25	73
50	10

Table 5
The particle counting test results on LS samples collected after the purification by the stripping plant.

Particle counting on stripping plant samples	
Particle size (μm)	Count/L
0.1	1200
0.15	500
0.2	100
0.3	0
0.5	0

with the ones shown in Table 4, i.e. the Class 50 level of the MIL-STD 1246C [33], adopted as the standard reference in JUNO. For each particle size, the number of particles present in the sample must not exceed the threshold value. In Table 5, the results of the tests on samples collected immediately after the stripping plant are reported. The sensitivity of the instrument is much higher than required by the Class 50 standard; nonetheless, the counts for the largest particles detected (0.3 and 0.5 μm) in the samples are already 0, whereas for Class 50 requirements the smallest particle size to be monitored is 5 μm and the counts should be <1660. This clearly demonstrates an excellent cleanliness level of all main components and an efficient filtration system.

Other QA/QC[4] measurements are still ongoing to fully characterize the purified samples after each step of the purification sequence, exploiting advanced techniques and pushing their sensitivity and detection limit to values beyond the state of the art. After a long phase of R&D, they have been optimized, refined, and validated. Their preliminary results on several purified LS samples seem very promising in terms of LS quality and purification and they will be released soon.

[4] Quality Control and Quality assurance.

5. Conclusion

This paper summarizes the design, main features and operation of the distillation and gas stripping purification plants, which have been built and installed at the JUNO site for the purification of the LAB-based liquid scintillator for the JUNO experiment. Thanks also to a preliminary test campaign at the Daya Bay laboratories, both these processes have been proven crucial for the accomplishment of the optical and radiopurity JUNO requirements, which are mandatory for its scientific program. The layout and design of the plants were driven by precise technical needs, including low background, cleanliness level, leak tightness and safety.

The plants have been recently commissioned and successfully tested to prepare the 6-month filling phase of the JUNO detector. Preliminary results show very effective purification performance and stable operating conditions of the plants.

Declaration of competing interest

The authors declare that they have no known competing financial interests or personal relationships that could have appeared to influence the work reported in this paper.

Acknowledgments

This work is funded by the Istituto Nazionale di Fisica Nucleare (INFN), Italy, through the JUNO experiment. Special thanks go to Michele Montuschi, for his key contributions to the development of the DCS control system; Mario Masetto, Eleonora Canesi, Gabriele Milone and the Polaris staff for their work on the pilot and full-scale purification plants; and to the Chinese colleagues Hu Tao, Zhou Li, Yu Boxiang, Cai Xiao, Fang Jian, Sun Lijun, Sun Xilei, Xie Yuguang, Ling Xin, Han Hechong and Huang Jinhao from IHEP for their invaluable help and support during the plant operation onsite.

References

[1] G. Bellini, et al., Borexino Collaboration, Neutrinos from the primary proton–proton fusion process in the Sun, Nature 512 (2014) 383–386, http://dx.doi.org/10.1038/nature13702.
[2] A. Gando, et al., KamLAND Collaboration, Reactor on-off antineutrino measurement with KamLAND, Phys. Rev. D 8 (2013) http://dx.doi.org/10.1103/PhysRevD.88.033001.
[3] F.P. An, et al., Observation of electron-antineutrino disappearance at Daya Bay, Phys. Rev. Lett. 108 (2012) http://dx.doi.org/10.1103/PhysRevLett.108.171803.
[4] J.H. Choi, et al., RENO Collaboration, Observation of energy and baseline dependent reactor antineutrino disappearance in the RENO experiment, Phys. Rev. Lett. 116 (2016) http://dx.doi.org/10.1103/PhysRevLett.116.211801.
[5] A. Abusleme, et al., JUNO Collaboration, JUNO physics and detector, Prog. Part. Nucl. Phys. 123 (2022) 103927, http://dx.doi.org/10.1016/j.ppnp.2021.103927.
[6] V. Albanese, et al., SNO+ Collaboration, The SNO+ Experiment, J. Instrum. 16 (2021) P08059, http://dx.doi.org/10.1088/1748-0221/16/08/P08059.
[7] A. Abusleme, et al., JUNO Collaboration, The JUNO experiment top tracker, Nucl. Instrum. Methods Phys. Res. A (2023) 168680, http://dx.doi.org/10.1016/j.nima.2023.168680.
[8] A. Abusleme, et al., JUNO Collaboration, Sub-percent precision measurement of neutrino oscillation parameters with JUNO, Chin. Phys. C 46 (2022) 123001, http://dx.doi.org/10.1088/1674-1137/ac8bc9.
[9] A. Abusleme, et al., JUNO Collaboration, Feasibility and physics potential of detecting ^{8}B solar neutrinos at JUNO, Chin. Phys. C 45 (2021) 023004, http://dx.doi.org/10.1088/1674-1137/abd92a.
[10] A. Abusleme, et al., JUNO Collaboration, Real-time monitoring for the next core-collapse supernova in JUNO, J. Cosmol. Astropart. Phys. 01 (2024) 057, http://dx.doi.org/10.1088/1475-7516/2024/01/057.
[11] A. Abusleme, et al., JUNO Collaboration, JUNO sensitivity on proton decay p → νK^{+} searches, Chin. Phys. C 47 (11) (2023) 113002, http://dx.doi.org/10.1088/1674-1137/ace9c6.
[12] A. Abusleme, et al., JUNO Collaboration, JUNO sensitivity to the annihilation of MeV dark matter in the galactic halo, J. Cosmol. Astropart. Phys. 09 (2023) 001, http://dx.doi.org/10.1088/1475-7516/2023/09/001.
[13] A. Abusleme, et al., JUNO Collaboration, Radioactivity control strategy for the JUNO detector, J. High Energy Phys. 11 (2021) 102, http://dx.doi.org/10.1007/JHEP11(2021)102.

[14] P. Huang, et al., Theoretical study of UV–Vis light absorption of some impurities in alkylbenzene type liquid scintillator solvents, Theor. Chem. Acc. 129 (2011) 229–234, http://dx.doi.org/10.1007/s00214-011-0926-8.
[15] A. Abusleme, et al., JUNO Collaboration, Optimization of the JUNO liquid scintillator composition using a Daya Bay antineutrino detector, Nucl. Instrum. Methods Phys. Res. A 988 (2021) 164823, http://dx.doi.org/10.1016/j.nima.2020.164823.
[16] M.R. Anderson, et al., SNO+ Collaboration, Development, characterisation, and deployment of the SNO+ liquid scintillator, J. Instrum. 16 (2021) P05009, http://dx.doi.org/10.1088/1748-0221/16/05/P05009.
[17] W. Beriguete, et al., Production of a gadolinium-loaded liquid scintillator for the Daya Bay reactor neutrino experiment, Nucl. Instrum. Methods Phys. Res. A 763 (2014) 82–88, http://dx.doi.org/10.1016/j.nima.2014.05.119.
[18] A. Abusleme, et al., JUNO Collaboration, JUNO sensitivity to ^{7}Be, pep, and CNO solar neutrinos, J. Cosmol. Astropart. Phys. 10 (2023) 022, http://dx.doi.org/10.1088/1475-7516/2023/10/022.
[19] H.S. Zhang, M. Beretta, et al., Refractive index in the JUNO liquid scintillator, Nucl. Instrum. Methods Phys. Res. A 1068 (2024) 169730, http://dx.doi.org/10.1016/j.nima.2024.169730.
[20] J. Benziger, et al., A scintillator purification system for the Borexino solar neutrino detector, Nucl. Instrum. Methods Phys. Res. A 587 (2008) 277, http://dx.doi.org/10.1016/j.nima.2007.12.043.
[21] Y. Kishimoto, Liquid scintillator purification, AIP Conf. Proc. 785 (2005) 193–198, http://dx.doi.org/10.1063/1.2060471.
[22] H. Ikeda, Purification of KamLAND-Zen liquid scintillator, AIP Conf. Proc. 1549 (2013) 197–200, http://dx.doi.org/10.1063/1.4818107.
[23] R. Ford, A scintillator purification plant and fluid handling system for SNO+, in: AIP Conf. Proc., Vol. 1672, 2015, 080003, http://dx.doi.org/10.1063/1.4927998.
[24] M. Agostini, et al., Borexino Collaboration, Simultaneous precision spectroscopy of pp,^{7}Be, and pep solar neutrinos with Borexino Phase-II, Phys. Rev. D 100 (2019) 082004, http://dx.doi.org/10.1103/PhysRevD.100.082004.
[25] C. Landini, Purification strategy of the JUNO liquid scintillator, Zenodo (2024) http://dx.doi.org/10.5281/zenodo.13468896.
[26] Z. Zhu, B. Yu, et al., Optical purification pilot plant for JUNO liquid scintillator, Nucl. Instrum. Methods Phys. Res. A 1048 (2023) 167890, http://dx.doi.org/10.1016/j.nima.2022.167890.
[27] X. Sun, Mixing and purification of master solution for JUNO, Zenodo (2024) http://dx.doi.org/10.5281/zenodo.13684977.
[28] J. Ye, J. Fang, et al., Development of water extraction system for liquid scintillator purification of JUNO, Nucl. Instrum. Methods Phys. Res. A 1027 (2022) 166251, http://dx.doi.org/10.1016/j.nima.2021.166251.
[29] P. Lombardi, et al., Distillation and stripping pilot plants for the JUNO neutrino detector: Design, operations and reliability, Nucl. Instrum. Methods Phys. Res. A 925 (2019) 6–17, http://dx.doi.org/10.1016/j.nima.2019.01.071.
[30] R. Treybal, Mass-Transfer Operations, third ed., McGraw-Hill Book Co., Singapore, 1981.
[31] X. Ling, et al., JUNO high purity nitrogen plant, Nucl. Instrum. Methods Phys. Res. A 208 (2024) 111305, http://dx.doi.org/10.1016/j.apradiso.2024.111305.
[32] T.Y. Guan, et al., Development of low-radon ultra-pure water for the Jiangmen Underground Neutrino Observatory, Nucl. Instrum. Methods Phys. Res. A 1063 (2024) 169244, http://dx.doi.org/10.1016/j.nima.2024.169244.
[33] Military Standard : Product Cleanliness Levels and Contamination Control Program, U.S. Department of Defence, https://snebulos.mit.edu/projects/reference/MIL-STD/MIL-STD-1246C.pdf.